Proc. Natl. Acad. Sci. USA
Vol. 88, pp. 11052–11056, December 1991
Neurobiology

Completely functional double-barreled chloride channel expressed from a single *Torpedo* cDNA

(electric organ/*Xenopus* oocyte/patch clamp/voltage-gated channel/reconstitution)

CHRISTIANE K. BAUER*, KLAUS STEINMEYER†, JÜRGEN R. SCHWARZ*, AND THOMAS J. JENTSCH†

*Physiologisches Institut and †Zentrum für Molekulare Neurobiologie (ZMNH), Universität Hamburg, Martinistrasse 52, D-2000 Hamburg 20, Federal Republic of Germany

Communicated by Bertil Hille, September 13, 1991 (received for review June 27, 1991)

ABSTRACT **We have performed an electrophysiological analysis of the recently cloned *Torpedo marmorata* Cl^- channel. Functional expression of Cl^- channels in oocytes of *Xenopus laevis* previously injected with cRNA yielded an outward-rectifying current activated by hyperpolarization. Replacement of Cl^- with other anions significantly reduced or inhibited the current. Single-channel recordings from cell-attached patches exhibited burst-like Cl^- channel activity with rapid fluctuations between three equally spaced substates (0 pS, 9 pS, and 18 pS). The properties of the cloned Cl^- channel were almost identical to those of the reconstituted native *T. californica* Cl^- channel and were in full agreement with the predictions of the double-barreled channel model [Hanke, W. & Miller, C. (1983) *J. Gen. Physiol.* 82, 25–45]. Our results imply that the cloned cDNA codes for the completely functional *Torpedo* electroplax Cl^- channel.**

Plasma membrane Cl^- channels play an important role in various cellular functions such as regulation of cell volume, transepithelial transport, and control of excitability (1). Although dysfunction of Cl^- channels has been implicated in diseases such as cystic fibrosis and myotonia, a scarcity of information exists on their molecular structure. Recently the primary structure of the Cl^- channel from the electric organ of *Torpedo marmorata* was obtained by cloning its cDNA through an expression cloning approach (2). Extensive biophysical studies on the *T. californica* Cl^- channel, performed in the lipid bilayer system by Miller and colleagues (3–5), provided strong evidence for the existence of a functionally dimeric channel. Its single-channel properties are well described by the "double-barreled" channel model, although the assumption of equivalence and independence of two protochannels (barrels) forming an entire channel is undoubtedly a simplification (5, 6). The entire channel is slowly activated (within seconds) upon hyperpolarization [the cis side of the bilayer corresponds to the intracellular side (2)]. In the activated state, the channel exhibits bursts during which the two protochannels rapidly open and close independently of each other. The protochannel open-probability increases with depolarization, but with sustained depolarization the entire channel complex deactivates. Thus the channel has at least two gates with different kinetics and inverted voltage dependence (5).

Previous measurements of macroscopic currents in cRNA-injected oocytes were compatible with these complex gating processes (2). However, it was still an open question whether the protein encoded by the cDNA was sufficient to give rise to the complex behavior as observed in single-channel recordings of the native channel reconstituted into lipid bilayers; e.g., there might have been a missing subunit. The main purpose of the present study was to resolve this issue with patch clamp measurements in cRNA-injected oocytes.

Our experiments show that Cl^- channels expressed in *Xenopus laevis* oocytes previously injected with cRNA derived from *T. marmorata* Cl^- channel cDNA are indistinguishable from the native Cl^- channels of *T. californica* as regards ion selectivity, single-channel conductance, and voltage dependence. Thus a single polypeptide (either alone or in a homooligomeric complex) is sufficient to generate the complex apparent double-barreled structure of the *Torpedo* electroplax Cl^- channel.

MATERIALS AND METHODS

Oocyte Expression. Capped synthetic RNA was synthesized using T3 RNA polymerase (Stratagene capping kit) and plasmid 7I34 (2) after linearization with *Xba* I and was taken up in diethyl pyrocarbonate-treated water. Oocytes from *X. laevis* were injected with about 50 nl of aqueous RNA solution by standard procedures (7). Between 4 and 200 ng of cRNA was injected in different experiments. Oocytes were kept at 18°C for 1–7 days before use in electrophysiological experiments.

Electrophysiological Measurements. *Voltage clamp experiments.* Standard two-microelectrode voltage clamp procedures were used to measure whole-cell membrane currents in oocytes. The oocytes were superfused with Ringer solution (116 mM NaCl/2 mM KCl/1.8 mM $CaCl_2$/1 mM $MgCl_2$/10 mM Hepes, pH 7.2) or a test solution (96 mM NaCl/2 mM KCl/1.8 mM $CaCl_2$/1 mM $MgCl_2$/5 mM Hepes, pH 7.6), which was modified by replacing part (50 mM) of the Cl^- by either Br^-, I^-, SCN^-, or cyclamate.

Patch clamp experiments. Oocytes were mechanically skinned of their vitelline membranes in a hypertonic solution (8) and then placed into the recording dish containing either normal frog Ringer solution or K^+ Ringer (Na^+ replaced by K^+). Patch pipettes (2.5 or 7 MΩ) were filled with the same solution as the bath solution.

All experiments were performed at room temperature. Stimulation and data acquisition were carried out with CED software (Cambridge Electronic Design, Cambridge). Data were low-pass-filtered (1 kHz or 300 Hz) and sampled at 0.1 kHz or, for single-channel data, at 1 kHz. An EPC7 patch clamp amplifier (List Electronics, Darmstadt, F.R.G.) was used.

Double-Barreled Channel Model Parameters. The following equations, given by Hanke and Miller (3), were used to perform the statistical analysis. The reaction scheme

$$S0 \underset{\mu}{\overset{2\lambda}{\rightleftharpoons}} S1 \underset{2\mu}{\overset{\lambda}{\rightleftharpoons}} S2 \qquad [1]$$

gives the transitions between the three substates of the activated double-barreled Cl^- channel, S0 (nonconducting),

The publication costs of this article were defrayed in part by page charge payment. This article must therefore be hereby marked "*advertisement*" in accordance with 18 U.S.C. §1734 solely to indicate this fact.

Abbreviation: RP, relative potential.

S1 (one subunit open), and S2 (both subunits open), governed by the opening rate constant λ and the closing rate constant μ.

The activation probability p of a single subunit of the channel (during bursting activity) is defined by the frequencies f of the substates S1 and S2:

$$f_{S0} = (1 - p)^2; f_{S1} = 2p(1 - p); f_{S2} = p^2; \quad [2]$$

$$p = (f_{S1} + 2f_{S2})/2. \quad [3]$$

The mean dwell time τ in a substate depends on the rate constants:

$$\tau_{S0} = 1/2\lambda; \tau_{S1} = 1/(\lambda + \mu); \tau_{S2} = 1/2\mu. \quad [4]$$

The relations of protochannel open probability, dwell times, and rate constants are given in the equations

$$p/(1 - p) = \lambda/\mu \quad [5]$$

$$\lambda = 1/2\tau_{S0}; \mu = 1/2\tau_{S2} \quad [6]$$

$$\lambda = p/\tau_{S1}; \mu = (1 - p)/\tau_{S1}. \quad [7]$$

The voltage dependence of p is described as

$$p(V) = \{1 + \exp[-zF(V - V_0)/RT]\}^{-1}, \quad [8]$$

where V_0 is the half-saturation voltage, and z, the charge that moves across the membrane upon channel opening, was set equal to 1 (3).

RESULTS

Ion Selectivity. The *T. californica* Cl^- channel was found to be highly selective for Cl^- over other anions (9). Whereas only Br^- can pass the channel to an appreciable degree, I^- and SCN^- actually block it (10). We investigated whether the cloned *Torpedo* channel displays the same ion selectivity. Macroscopic current–voltage relationships of cRNA-injected oocytes were measured with the two-microelectrode voltage clamp technique. Since the channel is slowly activated by hyperpolarization (2), we first hyperpolarized the oocyte membrane to −120 mV for 10 s. The current response to a depolarizing voltage ramp was then used to determine current–voltage relationships both in uninjected controls (Fig. 1*A*) and in cRNA-injected oocytes (Fig. 1*B*). To test for qualitative ion selectivity, extracellular Cl^- was partially exchanged with 50 mM Br^-, I^-, SCN^-, or cyclamate.

With control oocytes, there was nearly no effect of anion substitution at voltages more negative than −60 mV, indicating a small Cl^- conductance. With increasing depolarization, however, there was an increase in the slope of the current response, probably mediated by the activation of the endogenous Ca^{2+}-dependent Cl^- channel (11–13). The apparent conductance sequence in native oocytes was $SCN^- > I^- > Br^- > Cl^-$.

As reported previously (2), the current of cRNA-injected oocytes was outward-rectifying in the presence of Cl^-. Partial substitution of Cl^- outside by other anions led to a decrease in overall current and to a shift of the reversal potential toward the more positive new Cl^- equilibrium potential. This indicates that Cl^- is the most permeant species. Using the substitution with presumably functionally inert cyclamate ions as a reference, larger currents were observed only with Cl^- and Br^-. A sizable decrease in conductance was observed with I^- and SCN^-, indicating that the latter ions block the channel. The block by I^- became more effective with depolarization, an effect compatible with I^- being driven into the channel pore by transmembrane voltage. Within the voltage range examined, the block by SCN^- was only slightly voltage-dependent, though this was somewhat obscured by the opposite effect of SCN^- on the endogenous Cl^- channel (Fig. 1*A*). Thus, the anion selectivity of the *Torpedo* Cl^- channel expressed in *Xenopus* oocytes agrees with that observed in reconstitution (4, 9).

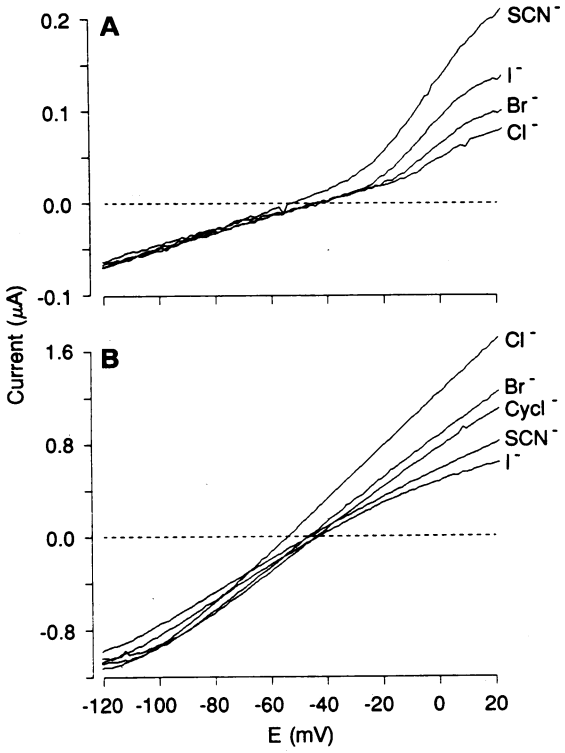

FIG. 1. Ion specificity of the expressed Cl^- channel. Whole-cell currents were measured with the two-microelectrode voltage clamp. (*A*) Control measurements in an uninjected oocyte. (*B*) Measurements in a cRNA-injected oocyte. Current responses during the positive slope of a voltage ramp (70 mV/s) were measured in normal and modified test solutions with 50 mM Cl^- replaced by an equimolar amount of the indicated anion. $Cycl^-$, cyclamate. The slope of the outward current represents the conductance of the external anion. Data were not corrected for leakage current.

Activation and Deactivation of Expressed Cl^- Current. The resting membrane potential of injected oocytes was usually between −30 and −20 mV. From a holding potential of −30 mV whole-cell current responses were elicited by two subsequent hyperpolarizing pulses. The newly expressed Cl^- current was activated by the first hyperpolarizing pulse (Fig. 2*A*). During the interstimulus interval of 5 s only part of the Cl^- conductance was deactivated. This accounts for the initial large Cl^- current at the beginning of the second pulse. The subsequent small current decrease during the hyperpolarization most probably represents the transition of activated channels from higher conductance levels at depolarizing potentials to lower conductance levels at more negative membrane potentials (4).

A similar pulse protocol was used to search for expressed Cl^- channels in cell-attached patches. In most patches no channel openings were observed except those of stretch-activated channels, which exhibited more or less spontaneous activity (14). In a few patches, extremely high "leakage" current was present, which changed direction close to a relative potential (RP) of 0 mV—i.e., near the oocyte resting membrane potential. The amplitude of this current slowly decreased with sustained depolarization and drastically increased upon the hyperpolarizing test pulses (Fig. 2*B*). The time course of activation and deactivation of this current was similar to that of the whole-cell current (Fig. 2*A*). This

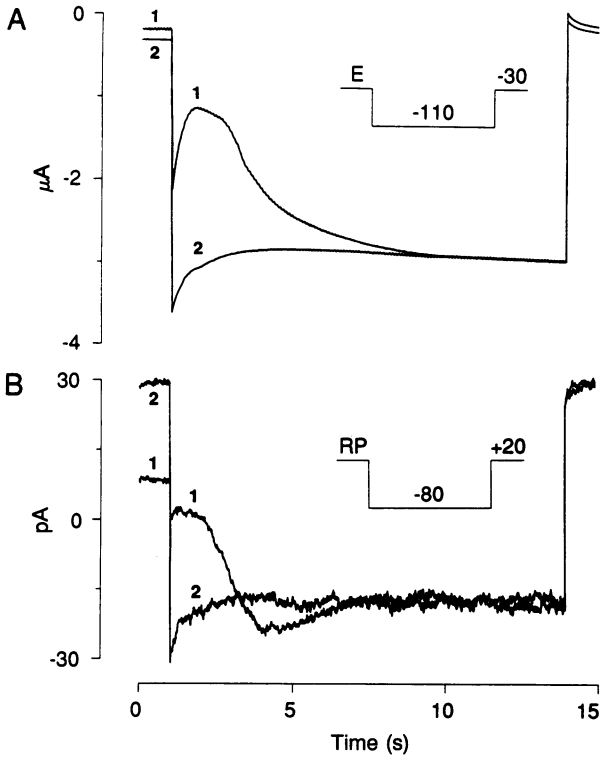

FIG. 2. Activation of expressed Cl^- conductance by hyperpolarization in cRNA-injected oocytes. (*A*) Whole-cell currents measured with the two-microelectrode voltage clamp. (*B*) Currents elicited by hyperpolarizing relative potentials (RP) in the cell-attached configuration. The numbers 1 and 2 near the current traces indicate the first and the second current response to two subsequent hyperpolarizing pulses. The interval between these pulses was 5 s. The last preceding stimulus pair was applied 2 min before. External solution, Ringer. Pulse protocol, see insets.

current could also be recorded with K^+ Ringer in the bath and pipette, suggesting that the hyperpolarization-activated inward current was carried by an efflux of Cl^- from the cytoplasm through newly expressed channels. In K^+ Ringer the change of current direction was shifted to slightly hyperpolarizing potentials, which is consistent with a depolarization of the oocyte membrane.

The fact that either no specific Cl^- currents or, in <5% of the patches, predominantly very large currents (ranging from several tens to several hundreds of pA) were recorded suggested that the newly expressed Cl^- channels were incorporated into the oocyte plasma membrane in clusters.

Single-Channel Recordings. In <1% of the cell-attached patches, activity of single newly expressed Cl^- channels was recorded that could easily be identified and distinguished from native channels by its activation behavior and single-channel characteristics. At RP = 0 mV, no channel openings were observed. Upon slow hyperpolarization the channel was activated between −50 mV and −70 mV RP. Fig. 3 shows bursts of single-channel activity at RP = −70 mV. The duration of bursts varied between 1 and 30 s and tended to decrease with prolonged hyperpolarization. Characteristically the channel rapidly fluctuated between three conductance levels during the burst, the lowest being equal to the closed state (0 pS).

According to the double-barreled channel model, the three conductance levels during a burst were defined as substates S0 (nonconducting), S1 (one channel subunit open), and S2 (both channel subunits open). The frequency of the channel being in a certain substate was voltage-dependent (Fig. 4). At RP = −30 mV, the channel was predominantly in the S2 substate, whereas substate S0 was more frequent with stronger hyperpolarizations. This is consistent with the macroscopic outward-rectifying properties of the *Torpedo* Cl^- channel. In Fig. 4, only hyperpolarizing potentials are shown because, in that experiment, depolarization caused the channel to stop bursting within seconds or several tens of seconds. Even at RP = −30 mV, the channel normally deactivated within <1 min. We did not further investigate these slow voltage-dependent activation and deactivation channel processes.

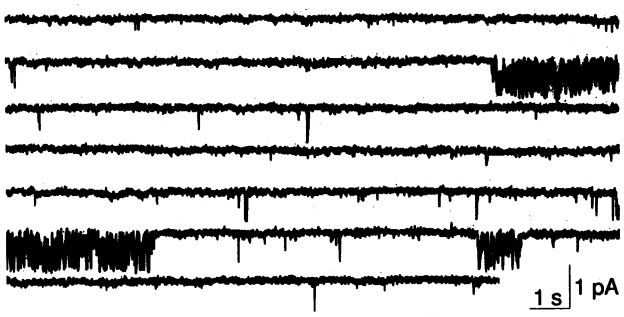

FIG. 3. Occurrence of bursts of single-channel activity recorded in the cell-attached mode after prolonged (>10 min) hyperpolarization to RP = −70 mV. During a burst, the channel rapidly fluctuates between three substates. External and pipette solution, Ringer.

Histograms of the single-channel current amplitude during bursts revealed that the substates are equally spaced. Fig. 5*A* shows an amplitude histogram of currents measured at RP = −90 mV with a superimposed fit of three Gaussian equations. Fig. 5*B* demonstrates the linear relationship between the mean current amplitude in the substates S1 and S2 and the RP. Linear regression analysis indicated chord conductances of 8.95 pS and 17.88 pS for the S1 and the S2 substate, respectively. For both substates, the extrapolated reversal potential was close to RP = 0 mV. Provided that the single-channel current was exclusively carried by Cl^-, this indicates that the membrane potential of the oocyte was nearly identical to the Cl^- equilibrium potential, as would be

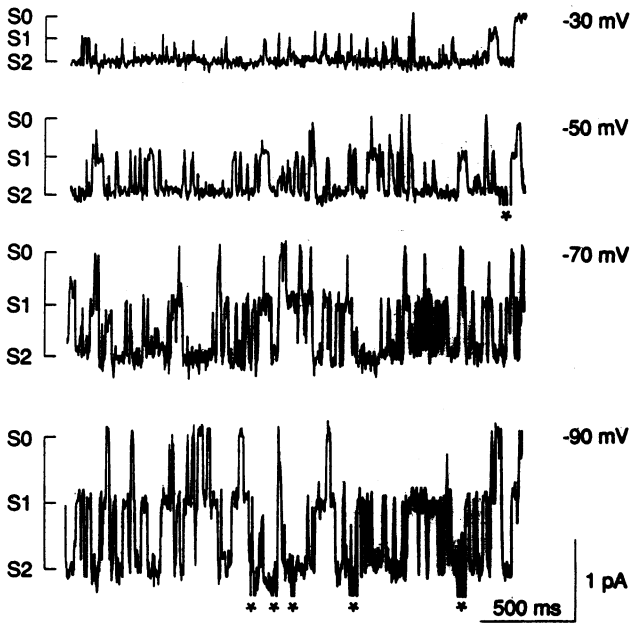

FIG. 4. Fluctuations of the newly expressed Cl^- channel between the substates S0, S1, and S2 during bursts recorded (cell-attached patch) at different relative potentials as indicated at the end of each current trace. With less-hyperpolarizing potentials, the channel is more frequently in the S2 substate. Stars indicate spontaneous openings of stretch-activated channels; the current trace is cut off at these positions. External solution, Ringer.

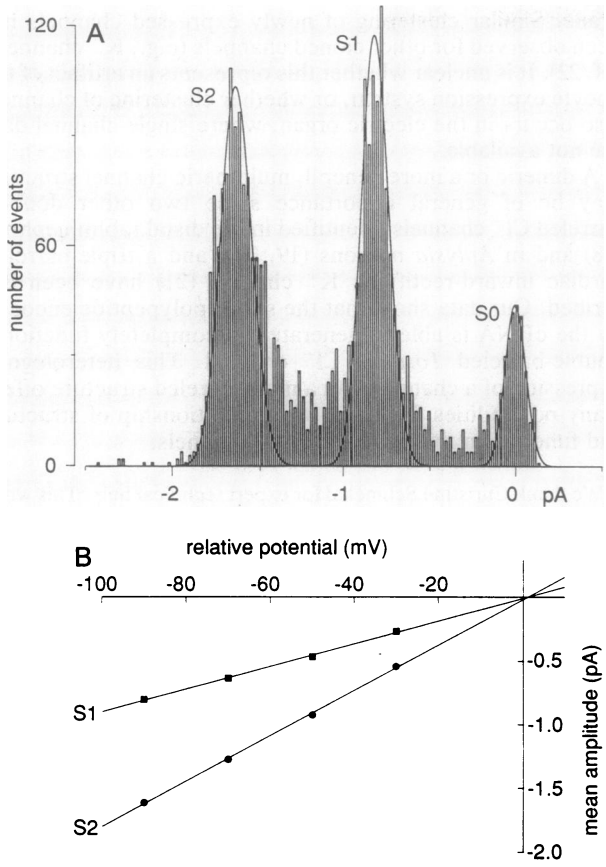

FIG. 5. (*A*) Distribution of current amplitude during bursts of channel activity at RP = −90 mV. Fit of three Gaussian curves to the data is superimposed. Mean current amplitude of the channel in substate S0 was equal to the mean current value between the bursts and was set equal to zero. The mean of the Gaussian fit to the current amplitude of S2 (−1.62 pA) is exactly twice the mean amplitude of S1 (−0.81 pA). This evaluation is from the experiment shown in Fig. 4. (*B*) Mean current amplitudes as determined by fits to amplitude histograms for the substates S1 and S2 in dependence of the relative potential. Lines are linear regressions to the data points and denote the chord conductance for the substates S1 (8.95 ± 0.26 pS, slope ± SE; r^2 = 0.998) and S2 (17.88 ± 0.37 pS; r^2 = 0.999).

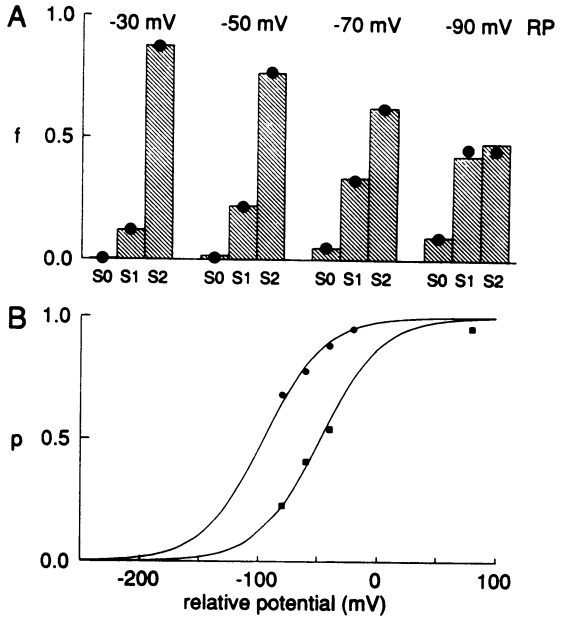

FIG. 6. Comparison of measured data with values predicted by the requirements of the double-barreled model. (*A*) Histogram of relative frequencies *f* of the three substates during bursts at the indicated potentials. Filled circles denote the experimental data, and hatched bars denote theoretical values according to Eq. 2. The activation probability *p* was directly determined as the time-averaged current in a burst divided by the mean current amplitude of the substate S2. (*B*) Dependence of the activation probability *p* on relative potential. ●, Data for the same experiment evaluated in *A*; ■, data of another experiment, where the voltage dependence of *p* was shifted to the right. The continuous curves are fits (least squares) to the two sets of data according to Eq. 8. V_0 = −105.47 mV (●) or −57.65 mV (■).

expected with a high acquired Cl^- conductance. The conductance of the subunits of the expressed Cl^- channel (each about 9 pS) was slightly smaller than that found in bilayer experiments (each about 10 pS), which might be due to the different concentrations of Cl^- in the reconstitution experiments (200 mM Cl^- on both sides) and in the oocytes.

Test of Double-Barreled Channel Model. The model of a double-barreled channel composed of two independently gating protochannels predicts a binomial distribution for the substate frequencies (4). This is indeed fulfilled for the reconstituted *T. californica* channel (3, 4), providing strong, but indirect evidence for the double-barreled channel model. We applied the same kind of analysis to the *T. marmorata* channel expressed from cRNA, using the equations given in *Materials and Methods*.

Substate frequencies *f* and activation probability *p* during bursts were evaluated in three different experiments. The distribution of substate frequencies during a burst was always found to be nearly identical to the binomial distribution required by the model. In Fig. 6*A*, measured substate frequencies (●) are compared with theoretical values (bars) calculated from Eq. 2. Protochannel activation probability *p* was determined by dividing the time-averaged current by twice the mean protochannel current. The activation probability *p* increased with less-hyperpolarizing potentials. Fig. 6*B* shows the voltage dependence of *p* from two different experiments. Each set of measured values for *p* could be described by a Boltzmann distribution (Eq. 8). The voltage dependence (given by the half-saturation values V_0 of −58 mV and −105 mV RP) differed greatly in these experiments. A possible explanation could be a variability of intracellular pH values in these experiments. A change of pH on the cis side by 1 unit has been found to shift the V_0 value by >60 mV in the bilayer experiments (3). In addition, membrane injury induces considerable local intracellular acidification in oocytes (15). This might also occur upon membrane stretch produced by the cell-attached patch electrode.

A further test of the model was the comparison of the mean dwell times τ in the three substates during a burst. RP = −90 mV was chosen to increase the frequency of substate S0. The values for τ shown in Table 1 are of the same order of magnitude as the data given by Hanke and Miller (3) for a membrane potential of −100 mV (low-pass filtering 0.5–1 kHz). Since the resting membrane potential of injected oocytes measured in Ringer solution was nearly always between −30 and −20 mV, a relative potential of −90 mV might correspond to an absolute potential of about −115 mV. This estimation allows a comparison with data obtained in the bilayer system. On the basis of the measured mean dwell times, the rate constants λ and μ were calculated independently in two different ways according to Eqs. 6 and 7. As required by the double-barreled model, the two methods gave similar values for the rate constants (Table 1). In addition, these values are in good agreement with the bilayer data given for membrane potentials of −100 mV and −120 mV (3).

DISCUSSION

Our results show that the properties of the newly expressed *T. marmorata* Cl^- channel are almost identical to those

Table 1. Measured and calculated values of several kinetic parameters predicted by the double-barreled channel model

Parameter(s)	Value(s)
Mean τ_{S0}, τ_{S1}, τ_{S2}	11.7, 16.4, 25.1 ms
f_{S0}, f_{S1}, f_{S2}	
Measured	0.09, 0.43, 0.48
Calculated (Eq. 2)	0.09, 0.42, 0.49
p (calculated, Eq. 3)	0.698
λ (calculated, Eqs. 6/7)	42.7/42.5 s^{-1}
μ (calculated, Eqs. 6/7)	19.9/18.4 s^{-1}

Mean τ, mean dwell time for the indicated substate; f, substate frequency; p, channel subunit activation probability; λ, opening rate constant; μ, closing rate constant.

reported for the reconstituted native *T. californica* Cl^- channel (5). This is true for properties of the macroscopic Cl^- currents such as the slow time course of activation and deactivation, the outward rectification, and the selectivity to various anions. In addition, at the single-channel level, the cloned Cl^- channel exhibited the same peculiar behavior as the native Cl^- channel. This is true for the burst-like activity with rapid fluctuations between three substates, the mean dwell times in these states, and the voltage dependence of the open probability for a single protochannel.

The single-channel properties described by the equations given by Hanke and Miller (3) agree well with the idea that the cloned *Torpedo* Cl^- channel consists of two identical independently gating protochannels. In fact, the three substate conductances were equally spaced (0 pS, 9 pS, and 18 pS) and the substate frequencies exhibited a nearly perfect binomial distribution.

The electrophysiological identity of the cloned channel expressed in oocytes to the one studied after reconstitution into lipid bilayers has two major implications. First, the double-barreled properties described for the *T. californica* channel (16) are not an artifact of reconstitution (there are no single-channel data available for intact tissue). Moreover, the lipid composition of the membrane does not seem to have profound effects on its single-channel conductance, a conclusion previously reached for the reconstituted channel (17). Second, and most important, the single protein encoded by the cloned cDNA (2) is sufficient to give rise to all biophysical properties examined. Thus both voltage-sensitive gates and the structures necessary for forming the postulated double-barreled channel must be present in this single polypeptide. We have no reason to suspect that we have missed a functionally important additional subunit, though we cannot exclude that additional proteins are associated with the channel *in situ*. Such proteins (e.g., cytoskeletal components) could possibly also be supplied by the oocyte.

It is essential to point out that the double-barrel model describes a functional homodimer (composed of two protochannels), which does not necessarily imply that it is a homodimer of two proteins encoded by the cloned cDNA. Each of the two protochannels could be an oligomer of two or more identical proteins. We cannot even rule out the possibility that a protein monomer generates the double-barreled characteristics, though we consider this to be highly unlikely. It will be important to clarify this issue (e.g., by chemical crosslinking of *Torpedo* membrane proteins).

As revealed by our patch clamp experiments, the *Torpedo* channel is expressed mostly in clusters in the oocyte membrane. Similar clustering of newly expressed channels has been observed for other cloned channels (e.g., K^+ channels; ref. 22). It is unclear whether this represents an artifact of the oocyte expression system, or whether clustering of channels also occurs in the electric organ, where single-channel data are not available.

A dimeric or a more general, multimeric channel structure may be of general importance since two other double-barreled Cl^- channels, identified in the distal rabbit nephron (18) and in *Aplysia* neurons (19, 20), and a triple-barreled cardiac inward-rectifying K^+ channel (21) have been described. Our data show that the single polypeptide encoded by the cDNA is able to generate the completely functional double-barreled *Torpedo* Cl^- channel. This heterologous expression of a channel with a multibarreled structure offers many possibilities for study of the relationship of structure and function in this novel class of channels.

We thank Christine Schmekal for expert technical help. This work was supported by grants of the Bundesministerium für Forschung und Technologie (to T.J.J.), the U.S. Cystic Fibrosis Foundation (to T.J.J.), and the Deutsche Forschungsgemeinschaft (to J.R.S.).

1. Frizzell, R. A. (1987) *Trends Neurosci.* **10**, 190–193.
2. Jentsch, T. J., Steinmeyer, K. & Schwarz, G. (1990) *Nature (London)* **348**, 510–514.
3. Hanke, W. & Miller, C. (1983) *J. Gen. Physiol.* **82**, 25–45.
4. Miller, C. (1982) *Philos. Trans. R. Soc. London Ser. B* **299**, 401–411.
5. Miller, C. & Richard, E. A. (1990) in *Chloride Channels and Carriers in Nerve, Muscle and Glial Cells*, eds. Alvarez-Leefmans, F. J. & Russell, J. M. (Plenum, New York), pp. 383–405.
6. Labarca, P., Rice, J. A., Fredkin, D. R. & Montal, M. (1985) *Biophys. J.* **47**, 469–478.
7. Colman, A. (1984) in *Transcription and Translation*, eds. Hames, B. D. & Higgins, S. J. (IRL, Oxford), pp. 271–300.
8. Methfessel, C., Witzemann, V., Takahashi, T., Mishina, M., Numa, S. & Sakmann, B. (1986) *Pflügers Arch.* **407**, 577–588.
9. White, M. M. & Miller, C. (1979) *J. Biol. Chem.* **254**, 10161–10166.
10. Miller, C. & White, M. M. (1980) *Ann. N.Y. Acad. Sci.* **341**, 534–551.
11. Barish, M. E. (1983) *J. Physiol. (London)* **342**, 309–325.
12. Boton, R., Dascal, N., Gillo, B. & Lass, Y. (1989) *J. Physiol. (London)* **408**, 511–534.
13. Miledi, R. (1982) *Proc. R. Soc. London Ser. B* **215**, 491–497.
14. Taglietti, V. & Toselli, M. (1988) *J. Physiol. (London)* **407**, 311–328.
15. Webb, D. J. & Nuccitelli, R. (1982) in *Intracellular pH: Its Measurement, Regulation, and Utilization in Cellular Functions*, eds. Nuccitelli, R. & Deamer, D. W. (Liss, New York), pp. 293–324.
16. Miller, C. & White, M. M. (1984) *Proc. Natl. Acad. Sci. USA* **81**, 2772–2775.
17. Miller, C. & White, M. M. (1981) *J. Gen. Physiol.* **78**, 1–18.
18. Sansom, S. C., La, B.-Q. & Carosi, S. L. (1990) *Am. J. Physiol.* **259**, F46–F52.
19. Chesnoy-Marchais, D. & Evans, M. G. (1986) *Pflügers Arch.* **407**, 694–696.
20. Chesnoy-Marchais, D. (1990) in *Chloride Channels and Carriers in Nerve, Muscle and Glial Cells*, eds. Alvarez-Leefmans, F. J. & Russell, J. M. (Plenum, New York), pp. 367–382.
21. Matsuda, H., Matsuura, H. & Noma, A. (1989) *J. Physiol. (London)* **413**, 139–157.
22. Stocker, M., Stühmer, W., Wittka, R., Wang, X., Müller, R., Ferrus, A. & Pongs, O. (1990) *Proc. Natl. Acad. Sci. USA* **87**, 8903–8907.